Temperature-dependent local structure in the Nb$_3$Ge superconductor studied by high-resolution Ge *K*-edge EXAFS measurements

N. L. Saini and M. Filippi

Unità INFM, Università di Roma "La Sapienza," Piazzale Aldo Moro 2, 00185 Roma, Italy

H. Oyanagi, H. Ihara, and A. Iyo

National Institute for Advanced Industrial Science and Technology, 1-1-1 Umezono, Tsukuba, Ibaraki 305-8568, Japan

A. Bianconi

Unità INFM and Dipartimento di Fisica, Università di Roma "La Sapienza," Piazzale Aldo Moro 2, 00185 Roma, Italy

Temperature dependent local structure of Nb$_3$Ge superconductor has been studied by Ge *K*-edge extended x-ray-absorption fine structure measurements. Correlated Debye-Waller factor of the Ge-Nb pairs shows a clear change across the superconducting transition temperature T_c. This change appears to be similar to the one observed for the high-T_c cuprates, indicating a common cause of pairing in the short coherence length superconductors. The results suggest an intimate relation between the local atomic displacements and the short coherence superconductivity, provoking models based on local electron-lattice interaction for the high-T_c superconductivity.

I. INTRODUCTION

Although electron-phonon interactions, the fundamental basis for the conventional superconductivity in metals, have been given minor importance to explain high-T_c superconductivity, recent experiments[1–3] support their active role in the characteristic properties of these complex copper oxides. Indeed, new models of superconductivity[4–6] in the high-T_c copper oxides seem to follow the emerging view of inhomogeneous electronic ground state of these materials with a significant role of electron-lattice interaction. The credit also goes to the studies aimed to reveal information on the local structure[7–10] since the local structure is expected to play a distinct role in the superconductivity with short coherence length (i.e., the case of high-T_c copper oxides). In addition, the recent discovery of superconductivity in a simple MgB$_2$ structure[11] has further ignited our interest to revisit the role of lattice excitations in the superconductivity even at higher temperature.

Here we have studied local structure of the Nb$_3$Ge superconducting system by extended x-ray-absorption fine structure (EXAFS). It is worth recalling that until the discovery of high-T_c superconductivity in the cuprates, the intermetallic compounds with *A*15-type structure were called high-T_c superconductors. The highest T_c was found in the Nb$_3$Ge system that belongs to the *A*15 structural family. The *A*15 superconductors have been widely studied in the past for their characteristic transport and structural properties.[12,13] Also the EXAFS, a tool of local and instantaneous displacements in the condensed matter,[14] was used to study the *A*15 compounds,[15–18] revealing some key information on their local structure. For example, Cargill *et al.*[15] used Nb *K*-edge EXAFS to study lattice dynamics using polycrystalline Nb$_3$Ge samples and found large anisotropic vibrational cor-

relations (much larger than other *A*15 structures as Nb$_3$Al, V$_3$Si, and Cr$_3$Si) related to the one-dimensional Nb-Nb chains. On the other hand, Brown *et al.*[18] used the Ge *K*-edge EXAFS to characterize Nb$_3$Ge thin films made by two different techniques.

In this paper we report evolution of the local structure of the Nb$_3$Ge in a temperature range of 6–300 K by high *k*-resolution fluorescence EXAFS, focusing in the region of superconducting transition temperature to explore possible role of local displacements. The Ge *K*-edge EXAFS reveals signature of a change in the correlated Debye-Waller factor of the Ge-Nb bonds at the superconducting transition temperature, similar to the case of high-T_c cuprate superconductors. This anomalous change across the T_c suggests an important role of local displacements for the superconductivity in the title compound.

II. EXPERIMENTAL DETAILS

Well-characterized thin film of Nb$_3$Ge superconductor, grown by the chemical vapor deposition on a sapphire substrate (film thickness ~2000 Å) was used for the measurements. The polycrystalline film shows a sharp superconducting transition ($\Delta T_c = 1$ K) below 20.6 K (Fig. 1). The resistance ratio $R_{300\,K}/R_{25\,K} \sim 2.4$ indicates the stoichiometric nature of the film (see, e.g., Ref. 19). The film was characterized by x-ray diffraction (XRD) before the measurements (see inset of Fig. 1). The main diffraction lines were well indexed by the *A*15 structure (space group $Pm3n$). The lattice parameter was determined to be 5.1398 Å (± 0.0007) by refinement of the XRD pattern, consistent with earlier structural studies on high-quality stoichiometric Nb$_3$Ge films.[19,20] There are some traces of a mi-
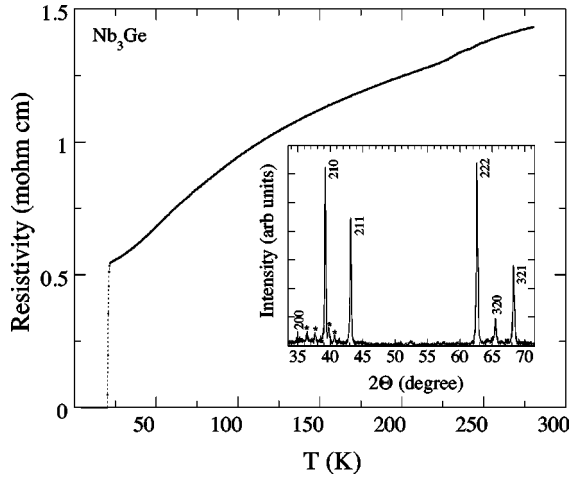
FIG. 1. Resistivity of the Nb_3Ge film as a function of temperature showing a sharp superconducting transition at a temperature of 20.6 K. The x-ray-diffraction (XRD) pattern of the Nb_3Ge thin film recorded at 300 K is shown as inset. The main peaks in the XRD correspond to a cubic structure with space group $Pm3n$. There are some extra weak peaks (marked with $\star$) due to small impurity of tetragonal phase Nb_5Ge_3, estimated to be $\sim4\%$.

nority phase (estimated to be $\sim4\%$) of Nb_5Ge_3 having tetragonal structure.[21]

The temperature-dependent Ge K-edge absorption measurements were performed in grazing incidence geometry at the beam line BL13B of the Photon Factory at the High Energy Accelerator Research Organization in Tsukuba. The synchrotron radiation emitted by a 27-pole wiggler source (maximum field B_0 of 1.5 T) inserted in the 2.5-GeV storage ring with a maximum stored current of 360 mA was monochromatized by a variable exit beam height double-crystal Si(111) monochromator and sagittally focused on the sample. Improvement of the storage ring and monochromator cooling system has been an added advantage for getting a stable x-ray beam on the sample. The spectra were recorded by detecting the fluorescence yield using a 19-element Ge x-ray detector array, covering a large solid angle of the x-ray fluorescence emission.[22] The emphasis was on measuring the spectra with a high signal-to-noise ratio, up to a high momentum transfer, and for that purpose we took several scans, with each scan averaged over 19 channels. The sample temperature was measured using a diode sensor attached to the sample plate, in the vicinity of the sample. The sample temperature was controlled within an accuracy of ±1 K using a standard controller based on the proportional, integral, and derivative (PID) algorithm. A standard procedure was used to extract the EXAFS signal from the absorption spectrum[14] and corrected for the x-ray fluorescence self-absorption before the analysis.[23]

III. RESULTS AND DISCUSSION

Figure 2 shows EXAFS oscillations at several representative temperatures measured using fluorescence yield mode on the thin film of the Nb_3Ge superconducting sample. The
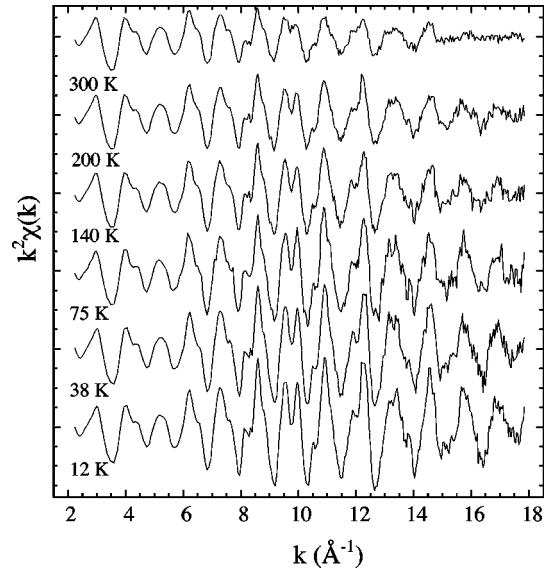

FIG. 2. EXAFS oscillations (multiplied by k^2) extracted from the Ge K-edge absorption spectra measured on Nb_3Ge at several representative temperatures.

EXAFS oscillations were extracted from the Ge K-edge absorption spectra and corrected for the fluorescence self-absorption. The EXAFS oscillations are weighted by k^2 to highlight the higher k region and the oscillations with high signal-to-noise ratio could be seen up to $k=18$ Å^{-1} even at high temperature. An overall damping of the EXAFS oscillations with increasing temperature is clear from the plots. The temperature-dependent behavior of the local structure could be better seen in the Fourier transform of the EXAFS oscillations providing a real-space information.

Figure 3 shows the Fourier transforms $|FT[k^2\chi(k)]|$ of the Ge K-edge EXAFS oscillations. The Fourier transforms (FT's) are performed between $k_{min}=3$ Å^{-1} and $k_{max}=18$ Å^{-1} using a Gaussian window and not corrected by the phase shifts due to the photoelectron backscattering to represent the raw experimental data. The FT represents the glo-
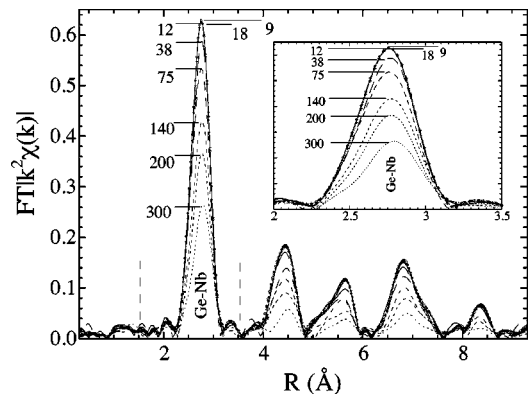

FIG. 3. Fourier transforms of the EXAFS spectra at several temperatures. The Fourier transforms have been performed at $k=3-18$ Å^{-1} using a Gaussian window and not corrected for the phase shifts. The inset shows an enlargement of the Ge-Nb FT peak. The vertical dashed lines are guide to the Fourier filtering range for the fit (see text).
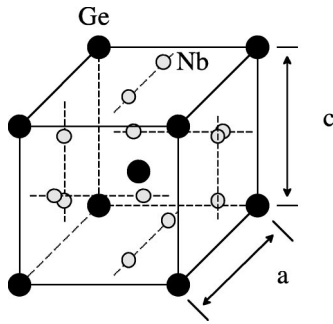
FIG. 4. Crystal structure of the Nb_3Ge system with black and white circles representing, respectively, the Ge and Nb atoms.

bal atomic distribution of the nearest neighbors around the absorbing Ge atom in the system. Here it is worth recalling that the Nb_3Ge crystal structure (see, e.g., Fig. 4) belongs to the $A15$ family. The Nb_3Ge lattice has Ge atoms at the bcc sites with Nb atoms in the pairs on the cubic faces, forming three sets of orthogonal chains in the extended structure. Near-neighbor distances from the Ge atoms in the structure are 2.88 Å (12 Nb atoms), 4.47 Å (8 Ge atoms), and 4.66 Å (12 Nb atoms), respectively, for the Ge-Nb, Ge-Ge, and Ge-Nb shells. Following the geometry around the photoabsorbing Ge, the main peak in the FT (Fig. 3) is denoted by Ge-Nb, representing the scattering of the ejected photoelectron at the Ge site with the nearest 12 Nb atoms. The peak between 4 and 5 Å corresponds to the Ge-Ge scattering, mixed with the contribution due to the next Ge-Nb shell. The peaks do not appear at the real atomic distances and the position should be corrected for the photoelectron backscattering phase shifts to find the quantitative value of the atomic positions with respect to the central Ge. Looking at the temperature dependence of the FT peaks we find an increase of intensity with decreasing temperature. This is clear from the inset of Fig. 3 where the enlargement of the Ge-Nb FT peak is shown, revealing the expected increase with decreasing temperature. The temperature dependence can be better seen in Fig. 5, where we have plotted the magnitude of the FT peaks due to the Ge-Nb bonds.
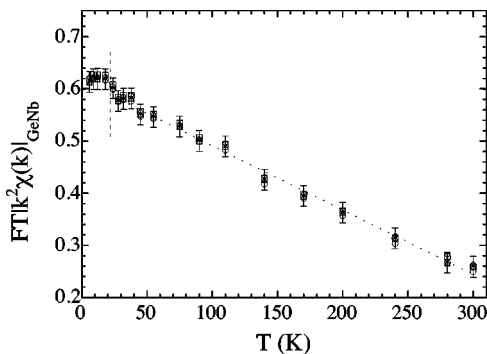

FIG. 5. Temperature dependence of the Ge-Nb Fourier transform (FT) peak for the Nb_3Ge system. Different symbols correspond to the peak intensities taken at different distances around the peak positions. The Ge-Nb FT peak intensity appears to shows a change across the T_c, indicated by a vertical dashed line. The dotted lines are guide to the eyes.

To have further insight into the local structure of the Nb_3Ge system as a function of temperature, focusing on the Nb-Nb chains around the Ge, we have analyzed the EXAFS spectra due to the Ge-Nb bonds. The signal of Ge-Nb bonds is well separated from the higher shells of other neighboring atoms and could be separately analyzed. The EXAFS amplitude depends on several factors as can be seen from the following general equation for EXAFS:[14]

$$\chi(k) = \sum_i N_i \frac{S_0^2}{kR_i^2} |f_i(k,R_i)| e^{-2R_i/\lambda} e^{-2k^2\sigma^2}$$

$$\times \sin[2kR_i + \delta_i(k)].$$

Here N_i is the equivalent number of neighboring atoms, at a distance R_i. S_0^2 is an amplitude correction factor due to photoelectron correlation (also called passive electron reduction factor), $f_i(k,R_i)$ is the backscattering amplitude, λ is the photoelectron mean free path, and σ^2 is the correlated Debye-Waller factor (DWF) of the photoabsorber-backscatterer pairs (Ge and Nb). Apart from these, the photoelectron energy origin E_0 and the phase shifts δ_i should be known. The above parameters can be either fixed or allowed to vary when an experimental EXAFS spectrum is parametrized. We have used the conventional procedure for the EXAFS analysis following diffraction studies as the starting point. In this approach the DWF include all distortion effects, taking into account both static and dynamic distortions.

We made an attempt to model the EXAFS by a single Ge-Nb distance as suggested by the diffraction studies, however, we could not obtain a satisfactory fit using either Gaussian or non-Gaussian approach. In addition, increase in the width of the Ge-Nb distribution suggested another coexisting Ge-Nb distance. In fact, a smaller Ge-Nb distance of $\sim$2.66 Å was indicated to coexist with the crystallographic distance of $\sim$2.88 Å in this system by an earlier EXAFS study.[18] This made us to use a starting model with two Ge-Nb distances. Introduction of the model with two Ge-Nb distances improved the fit index by $\sim$40% with respect to the model of one Ge-Nb distance.

The number of parameters which may be determined by EXAFS is limited by the number of independent data points: $N_{ind} \sim (2\Delta k\Delta R)/\pi$, where Δk and ΔR are, respectively, the ranges in k and R space over which the data are analyzed. In our case $\Delta k = 15$ Å^{-1} and $\Delta R = 2$ Å (see the vertical dashed lines in Fig. 3) give $N_{ind} \sim 20$ for the EXAFS due to the Ge-Nb shell.[14] In the present analysis, the effective amplitude reduction factor S_0^2 is fixed to 0.64, obtained by the best-fit results. Although it is in good agreement with the other Ge K-edge studies, reporting S_0^2 to be between 0.6 and 0.7,[24,25] a slightly lower value of the amplitude reduction factor could be due to preferred orientation of the thin film studied in this work. The best-fit value of the photoelectron energy origin E_0 was kept fixed at 4.2 eV above the Ge absorption jump value. Therefore, except the two Ge-Nb radial distances and corresponding DWF's, all other parameters were kept fixed in the conventional least-squares paradigm. Figure 6 shows representative fits for the isolated
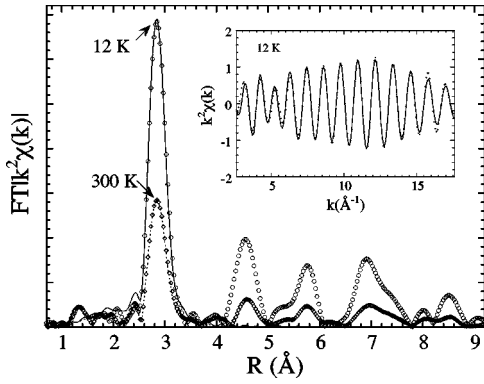
FIG. 6. Representative fits (solid line) to the Ge-Nb EXAFS (data points) at 12 K (solid line) and 300 K (dotted line) using two distances (see text). The isolated Ge-Nb EXAFS (multiplied by k^2) at 12 K is shown as inset with the fit.

Ge-Nb EXAFS using the two distances. While the shorter Ge-Nb distance ($\sim 2.66 \pm 0.01$ Å) shows a small but gradual increase with decreasing temperature, the longer bond remains temperature independent, $\sim 2.880 \pm 0.005$ Å, in the temperature range studied here. Relative probabilities of the two distances (1/3 and 2/3, respectively, for the short and long bonds) were found to be temperature independent within the experimental uncertainties.

Temperature dependence of the Debye-Waller factors of the Ge-Nb pairs, σ^2_{Nb1} and σ^2_{Nb2}, determined from the above analysis, are shown in Fig. 7. The uncertainties in the parameters were estimated by the standard EXAFS (parabola) method.[26-28] In this method, the quality of fit parameter, proportional to the statistical χ^2, is determined as a function of the concerned parameter. The uncertainties are usually estimated from a fractional increase δ of χ^2 above its minimum value. This fraction δ depends on several experimental and data analysis factors. In order to establish the reported uncertainties we have analyzed four independent EXAFS scans at each temperature.

The DWF's follow smooth behavior for both Ge-Nb bonds as a function of temperature, at least down to ~ 50 K. Below this temperature there seems some divergence from this smooth behavior. The temperature dependence could be fitted with an Einstein model with Einstein temperatures $T_E = 230$ K and $T_E = 210$ K, respectively, for the σ^2_{Nb1} and σ^2_{Nb2} with constant values (0.005 and 0.0017, respectively) for the zero-point energies. While the value of $T_E = 230$ K for the σ^2_{Nb1} is consistent with the earlier reports,[18,20] we find slightly different $T_E = 210$ K for the σ^2_{Nb2}.

There appears a divergence from the normal behavior of the DWF's with a small anomaly in the local structure at the T_c, which is more clear in the temperature dependence of the σ^2_{Nb2}. This interesting and anomalous change at the superconducting transition temperature appears to be similar to the one observed in the high-T_c cuprate superconductors by Cu K-edge EXAFS.[10] Incidentally, similar behavior, with a drop at T_c, was observed in the cuprate superconductors by ion channeling experiment.[7] In addition, the drop in the cuprates was found to depend on the critical temperature T_c, being larger while the T_c is higher. Figure 8 shows the rela-
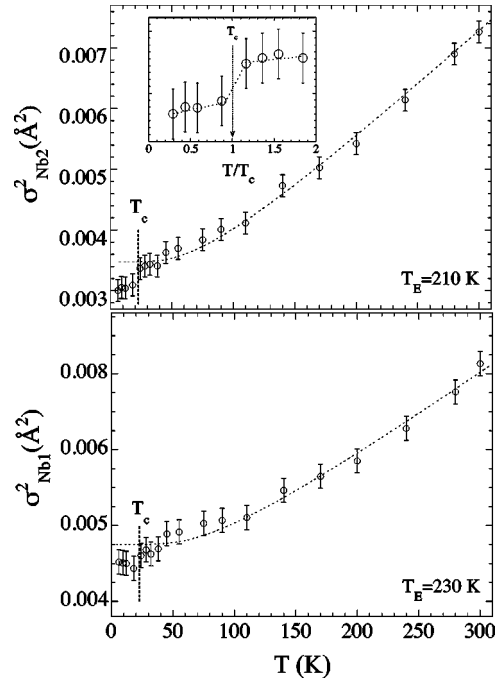

FIG. 7. Temperature dependence of the correlated Debye-Waller factors (symbols) of the Ge-Nb pairs, σ^2_{Nb1} (lower) and σ^2_{Nb2} (upper). The expected temperature dependence of the Debye-Waller factors for a fully correlated motion of Ge and Nb, calculated by Einstein model, are shown by the dotted lines. The σ^2_{Nb1} and σ^2_{Nb2} are well described by the Einstein model with $T_E = 230$ K and 210 K, respectively, above the T_c (see text). An enlarged view of the change at the T_c is shown in the inset as a function of normalized temperature.

tionship between the superconducting transition temperature and the value of the drop in the DWF ($\Delta\sigma^2$) at the T_c for the cuprates,[10] plotted with the drop in the DWF for the Nb$_3$Ge. While DWF for the Cu-O bonds are used, being the main electronic component, the DWF for the Ge-Nb is given considering the fact that the orthogonal Nb chains are the important structural elements for the electronic structure of the Nb$_3$Ge system. The T_c versus $\Delta\sigma^2$ appears to indicate some kind of relationship between the two parameters. At this stage it is rather hard to argue on the precise role of the local
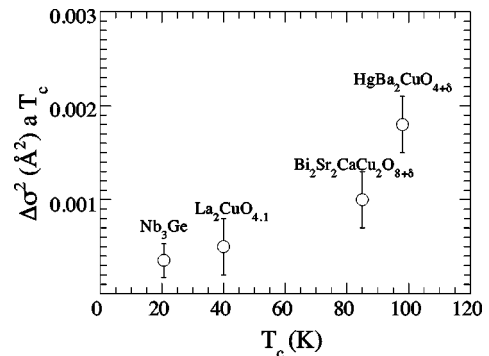

FIG. 8. Change in the Debye-Waller factors ($\Delta\sigma^2$) across the T_c vs the T_c for the cuprates (Ref. 10) is compared with the change for the Nb$_3$Ge.

lattice displacements, however, we think that the fundamental electronic band structure near the singularity point (M point in the cuprates and G point in the A15 intermetallics) could be modified by these small displacements.

It should be recalled that some of the A15 intermetallics show martensiticlike transition, at a temperature several kelvins above the T_c.[29] This transition is characterized by shortening of the Nb-Nb distance along one of the chains and an enlargement of the distance along the orthogonal chains. The instability has been studied by different experimental techniques,[13,29] however, the transition seems sample dependent and was observed mainly in the V_3Si and Nb_3Sn systems. We speculate that coexisting Ge-Nb distances observed in the present experiment may be a signature of martensiticlike phase in the Nb_3Ge system. Since no evidence was ever found for martensiticlike phase in the Nb_3Ge system using conventional experimental techniques, the phase may be existing only at a local scale. However, more efforts are needed to clarify the possibility of martensiticlike phase in the title system.

In summary, we have studied temperature-dependent local structure of the Nb_3Ge superconductor by the Ge K-edge EXAFS measurements. The local and instantaneous atomic displacements across the superconducting transition temperature, determined by the correlated Debye-Waller factor of the Ge-Nb bonds, indicate a small but clear divergence from their normal temperature dependence. The decrease of the DWF at the superconducting transition temperature T_c appears similar to the one found for the DWF of Cu-O bonds in the high-T_c cuprate superconductors. The results indicate that the local displacements are tied to the superconductivity of the materials with small coherence length. In conclusion, the results suggest importance of the local displacements in the superconductivity in the short coherence length superconductors as the doped cuprates and the A15 compounds. Therefore the experimental findings support the approach based on local electron-phonon interaction[30] to discuss the high-T_c in the A15 superconductors, resulting in an effective double-well potential and anharmonic phonon modes.

[1] A. Lanzara, P.V. Bogdanov, X.J. Zhou, S.A. Kellar, D.L. Feng, E.D. Lu, T. Yoshida, H. Eisaki, A. Fujimori, K. Kishio, J.-I. Shimoyama, T. Nodak, S. Uchida, Z. Hussain, and Z.-X. Shen, Nature (London) **412**, 510 (2001).

[2] A. Lanzara, G.-m. Zhao, N.L. Saini, A. Bianconi, K. Conder, H. Keller, and K.A. Müller, J. Phys.: Condens. Matter **11**, L541 (1999).

[3] D. Rubio Temprano, J. Mesot, S. Janssen, K. Conder, A. Furrer, H. Mutka, and K.A. Müller, Phys. Rev. Lett. **84**, 1990 (2000).

[4] A.H. Castro Neto, Phys. Rev. B **64**, 104509 (2001).

[5] S. Andergassen, S. Caprara, C. Di Castro, and M. Grilli, Phys. Rev. Lett. **87**, 056401 (2001), and references therein.

[6] S.R. Shenoy, T. Lookman, A. Saxena, and A.R. Bishop, Phys. Rev. B **60**, R12 537 (1999).

[7] R.P. Sharma, S.B. Ogale, Z.H. Zhang, J.R. Liu, W.K. Wu, B. Veal, A. Paulikas, H. Zhang, and T. Venkatesan, Nature (London) **404**, 736 (2000), and references therein.

[8] E.S. Bozin, G.H. Kwei, H. Takagi, and S.J.L. Billinge, Phys. Rev. Lett. **84**, 5856 (2000), and references therein.

[9] R.J. McQueeney, Y. Petrov, T. Egami, M. Yethiraj, G. Shirane, and Y. Endoh, Phys. Rev. Lett. **82**, 628 (1999), and references therein.

[10] N.L. Saini, A. Bianconi, and H. Oyanagi, J. Phys. Soc. Jpn. **70**, 2092 (2001), and references therein.

[11] J. Nagamatsu, N. Nakagawa, T. Muranaka, Y. Zenitani, and J. Akimitsu, Nature (London) **410**, 63 (2001).

[12] See, e.g., the general review on A15 materials by J. Müller, Rep. Prog. Phys. **43**, 641 (1980).

[13] See, e.g., a review on structural aspects of A15 materials by L.R. Testardi, Rev. Mod. Phys. **47**, 637 (1975).

[14] *X Ray Absorption: Principle, Applications Techniques of EXAFS,* *SEXAFS and XANES*, edited by R. Prinz and D. Koningsberger (Wiley, New York, 1988).

[15] G.S. Cargill, III, R.F. Boehme, and W. Weber, Phys. Rev. Lett. **50**, 1391 (1983).

[16] T. Claeson, J.B. Boyce, and T.H. Geballe, Phys. Rev. B **25**, 6666 (1982).

[17] J.B. Boyce, F. Bridges, T. Claeson, T.H. Geballe, G.W. Hull, N. Kitamura, and F. Weiss, Phys. Rev. B **37**, 54 (1988).

[18] G.S. Brown, L.R. Testardi, J.H. Wernick, A.B. Hallak, and T.H. Geballe, Solid State Commun. **23**, 875 (1977).

[19] L.R. Testardi, R.L. Meek, J.M. Poate, W.A. Royer, A.R. Storm, and J.H. Wernick, Phys. Rev. B **11**, 4304 (1975).

[20] G.W. Hull and L.R. Newkirk, J. Low Temp. Phys. **29**, 297 (1977); A.H. Dayem, T.H. Geballe, R.B. Zubeck, A.B. Hallak, and G.W. Hull, Jr., Appl. Phys. Lett. **30**, 541 (1977).

[21] S. Jagner and S.E. Rasmussen, Acta Crystallogr., Sect. B: Struct. Crystallogr. Cryst. Chem. **31**, 2881 (1975).

[22] H. Oyanagi, R. Shioda, Y. Kuwahara, and K. Haga, J. Synchrotron Radiat. **2**, 99 (1995); H. Oyanagi, *ibid.* **5**, 48 (1998).

[23] L. Tröger, D. Arvanitis, K. Baberschke, H. Michaelis, U. Grimm, and E. Zschech, Phys. Rev. B **46**, 3283 (1992).

[24] E.A. Stern, B.A. Bunker, and S.M. Heald, Phys. Rev. B **21**, 5521 (1980).

[25] L. Incoccia, S. Mobilio, M.G. Proietti, P. Fiorini, C. Giovannella, and F. Evangelisti, Phys. Rev. B **31**, 1028 (1985).

[26] G.G. Li, F. Bridges, and C.H. Booth, Phys. Rev. B **52**, 6332 (1995).

[27] Report of the International Workshop on Standards and Criteria in X-ray Absorption Spectroscopy, in Proceedings of the 5th International Conference on X-ray Absorption Fine Structure, edited by F. W. Lytle, D. E. Sayers, and E. A. Stern [Physica B **158**,

701 (1989)]; *Proceedings of the 6th International Conference on X-ray Absorption Fine Structure*, edited by S. Hasnain (Ellis Horwood, England, 1991), p. 751.

[28] R.W. Joyner, K.J. Martin, and P. Meehan, J. Phys. C **20**, 4005 (1987).

[29] J.B. Hastings, Y. Fujii, G. Shirane, and S.J. Williamson, Phys. Rev. B **28**, 322 (1983); K. Hirota, L. Rebelsky, and G. Shirane, *ibid.* **51**, 11 325 (1995).

[30] C.C. Yu and P.W. Anderson, Phys. Rev. Lett. **29**, 6165 (1984).